



HAL
open science

Congenital Infection of Severe Acute Respiratory Syndrome Coronavirus 2 With Intrauterine Fetal Death: A Clinicopathological Study With Molecular Analysis

Emmanuelle Lesieur, Julia Torrents, Frédéric Fina, Christine Zandotti, Julie Blanc, Sophie Collardeau-Frachon, Céline Gazin, Delphine Sirgant, Soraya Mezouar, Myriem Otmani Idrissi, et al.

► To cite this version:

Emmanuelle Lesieur, Julia Torrents, Frédéric Fina, Christine Zandotti, Julie Blanc, et al.. Congenital Infection of Severe Acute Respiratory Syndrome Coronavirus 2 With Intrauterine Fetal Death: A Clinicopathological Study With Molecular Analysis. *Clinical Infectious Diseases*, 2022, 75 (1), pp.E1092-E1100. 10.1093/cid/ciab840 . hal-03665773

HAL Id: hal-03665773

<https://amu.hal.science/hal-03665773v1>

Submitted on 22 Jan 2024

HAL is a multi-disciplinary open access archive for the deposit and dissemination of scientific research documents, whether they are published or not. The documents may come from teaching and research institutions in France or abroad, or from public or private research centers.

L'archive ouverte pluridisciplinaire **HAL**, est destinée au dépôt et à la diffusion de documents scientifiques de niveau recherche, publiés ou non, émanant des établissements d'enseignement et de recherche français ou étrangers, des laboratoires publics ou privés.

Copyright

Congenital infection of SARS-CoV-2 with intrauterine foetal death: a clinicopathological study with molecular analysis

Emmanuelle Lesieur ^{1,2}, Julia Torrents ¹, Frédéric Fina ^{1,3}, Christine Zandotti ⁴, Julie Blanc ^{5,6}, Sophie Collardeau-Frachon ⁷, Céline Gazin ⁴, Delphine Sirgant ⁸, Soraya Mezouar ⁴, Myriem Otmani Idrissi ⁴, Hubert Lepidi ¹, Florence Bretelle ^{2,9}, Jean-Louis Mege ⁴, Laurent Daniel ^{1,10}, Radia Fritih ¹

1. Department of Pathology and Neuropathology, La Timone Hospital, Aix Marseille University, Marseille, France

2. Prenatal Diagnosis Center, Department of Obstetrics and Gynaecology, La Conception Hospital, Aix Marseille University, Boulevard Baille, 13005 Marseille, France

3 ID Solutions, Grabels, France

4. IHU Méditerranée infection MEPHI - Aix-Marseille Université – 13005 Marseille, France - IRD – APHM

5. Department of Obstetrics and Gynaecology, Nord Hospital, APHM, Chemin des Bourrely, 13015, Marseille, France;

6. EA3279, CEReSS, Health Service Research and Quality of Life Center, Aix-Marseille University, 13284, Marseille, France.

7. Institut de Pathologie Multisite, Groupement Hospitalier Est, Hospices Civils de Lyon, France; Université Claude Bernard Lyon 1, France.

8. Department of Obstetrics and Gynaecology, Ste Musse Hospital, 54, rue Henri Sainte Claire Deville, 83000, Toulon, France

9. *Aix-Marseille Université, Unité de Recherche sur les Maladies Infectieuses Tropicales et Emergentes, UM63, CNRS 7278, IRD 198, INSERM 1095, Marseille, France.*

10. *Aix Marseille University - INSERM 1263 - INRAE 1260, France*

Correspondence

Dr. Emmanuelle Lesieur, Prenatal Diagnosis Center, Department of Obstetrics and Gynaecology, La Conception Hospital, Aix Marseille University, Boulevard Baille, 13005 Marseille. Phone: + 33 491 384 257, mail: Emmanuelle.lesieur@ap-hm.fr

Summary

From a case of in utero foetal death at 24⁺² weeks of gestation that occurred two days after the diagnosis of symptomatic SARS-CoV-2 infection in the mother, we isolated the incriminating virus by immunochemistry and molecular techniques in several foetal tissues, with a variant analysis of the SARS-CoV-2 genome.

Accepted Manuscript

Abstract

Observations of vertical transmission of SARS-CoV-2 infection from mother to foetus have recently been described in the literature. However, the consequences of such transmission, whether foetal or neonatal, are poorly understood. From a case of in utero foetal death at 24⁺² weeks of gestation that occurred seven days after the diagnosis of symptomatic SARS-CoV-2 infection in the mother, we isolated the incriminating virus by immunochemistry and molecular techniques in several foetal tissues, with a variant analysis of the SARS-CoV-2 genome. Moreover, the foetal demise could be explained by the presence of placental histological lesions, such as histiocytic intervillitis and trophoblastic necrosis, in addition to foetal tissue damage. We observed mild foetal growth retardation and visceral damage to the liver, causing hepatocellular damage and haemosiderosis. To the best of our knowledge, this is the first report in the literature of foetal demise secondary to maternal-foetal transmission of SARS-CoV-2 with a congenital infection and a pathological description of placental and foetal tissue damage. SARS-CoV-2 was identified in both specimens by three independent techniques (immunochemistry, RT-qPCR and RT-dPCR). Furthermore, the incriminating variant has been identified.

Keywords

In utero foetal death – Miscarriage – SARS-CoV-2 – congenital infection

Introduction

Pregnancy is associated with a higher risk of severe SARS-CoV-2 infection than that in the nonpregnant population (1,2). The risk of vertical transmission and its possible consequences have already been studied (3–5). Thus, it was only recently shown that vertical transmission from the mother to foetus was possible. Although some authors pointed out that the risk of miscarriage did not appear to be increased in infected women (6), the possibility of an unfavourable pregnancy outcome, such as intrauterine foetal death (IUD), secondary to SARS-CoV-2 infection remains unresolved. The diagnosis and identification of a variant would also be questions raised by such a possibility. Here, we present the adverse outcome of an intrauterine infection of SARS-CoV-2 causing foetal demise and placental and foetal injuries, with the identification of viral RNA and proteins in both specimens in addition to detection of the incriminating variant.

Case study

A 40-year-old woman, gravida 3, para 2, was admitted to the maternity emergency unit in February 2021 at 24⁺² weeks of gestation (WG) for decreased active foetal movements. The patient already had two healthy children born at term from uncomplicated pregnancies and only had a history of hypothyroidism that was stable and treated for 10 years with L-thyroxin. The pregnancy was uneventful, and all ultrasound examinations and routine tests were normal. A mid-trimester ultrasound was performed 2 weeks earlier and was normal.

Six days before her admission, she presented with a severe cough without fever. Real-time polymerase chain reaction (RT-qPCR) testing of SARS-CoV-2 was positive on her nasopharyngeal swabs, which allowed the detection of 20H/501Y. V2 (B1.351, Beta) variant.

On arrival at the department, the patient was haemodynamically stable, had good oxygen saturation (99%), and did not have a fever (36°1); her respiratory rate was 19 cycles/minute. Routine laboratory tests revealed thrombocytopenia of 100.000 G/L, and her haemoglobin was 11.5 g/dl. The

ultrasound showed a 550 g foetus with only a few movements, normal amniotic fluid and normal placental morphology and umbilical Doppler. The foetal heart rate was 150 bpm, which was normally oscillating and reactive for the term. Ultrasound and follow-up monitoring were then recommended, without indication for hospitalization. The next day, the patient presented with blood loss and decreased foetal movements. On ultrasound, foetal cardiac activity was not found, leading to the diagnosis of an IUD. The ultrasound appearance of the placenta was unremarkable, with normal amniotic fluid. The medical assessment carried out in the patient 24 hours prior showed that the patient was stable (111,000 G/L platelets, normal coagulation and hepatic assessment). It was decided to induce labour, which delivered a stillborn female weighing 528 g. A pathological examination of the foetus and placenta was offered and approved by the couple.

Materials and Methods

Pathological examination

Foetal autopsy and placental sampling and grossing were performed according to recommendations of the French Society of Fetopathology (7). Body parameters and fresh organ weights were evaluated according to Maroun and Graem growth curves.

Microscopic examination was carried out for foetal and placental tissues fixed in 4% buffered formalin, and samples were paraffin embedded (FFPE). Staining methods performed on 3–5 µm thick sections were haemalun eosin saffron, Perls Prussian blue (thymus, lung, bronchial tree, stomach, spleen, adrenal gland, kidney, oesophagus, liver, heart, pancreas, and trachea), Trichrome (liver and heart) and Reticulin (liver) stains.

IHC with peroxidase detection and haemalun counterstain was performed in a Ventana BenchMark XT and Ventana BenchMark ULTRA automat using the ultra-View Universal DAB Detection kit after heat pretreatment at pH 6 or 9 depending on the monoclonal antibodies tested: CD163 (Leica 10D6,

1:250), CD20 (Cliniscience L26, 1/150), CD3 (Dako F7.2.38, polyclonal ready to use), CD8 (DAKO CD8/144B, 1:1000), CD4 (Roche SP35 ready to use), MUM1(DAKO Mum1P, 1:25), CD68 (Menarini KP1, 1/200), AE1-AE3 (Roche polyclonal ready to use), HSV1 (DAKO poly, 1/500, HSV2 (Diagnostics, poly, ready to use), PAVOVIR9 (KO, polyclonal B150), CMV1 (B1.8KO, 1/500, HSV2 (Clinostics, 4C4C4, ready to use), and PAVOVIR9 (R9:100). C5b-9 and C4d were used as negative controls on foetal (liver and lung) and placental specimens with similar preanalytic conditions. The identification of C5b-9 and C4d within some of the decidual cells and in a number of villi and perivillous fibrin deposition were considered nonspecific staining.

SARS-CoV-2 (ProSci, 2019-nCoV Envelope antibody, rabbit pAB,1:100), SARS-CoV-2 (RDS, SARS-CoV-2 Spike S1, monoclonal mouse, 1:10). Negative controls (placenta and foetal liver specimens) were included for SARS-CoV-2 proteins with similar preanalytic conditions of formalin fixation. Immunohistochemistry (IHC) using anti-SARS-CoV-2 antibodies (anti-envelope and/or anti-spike proteins) was carried out on placental (extraplacental membranes, placental disk) and selected FFPE foetal specimens (lung, heart, liver and stomach).

RNA extraction

Paraffinized samples (one slide per tissue sampled) were pretreated with deparaffinization solution (QIAGEN), frozen samples were mashed, and all lysates were incubated with Proteinase K. After the addition of MS2 bacteriophage (as an extraction control), nucleic acid samples were extracted by EZ1 Virus Mini Kit v2.0 (QIAGEN) on an EZ1 automat (QIAGEN).

RT-qPCR for SARS-CoV-2

The extracts obtained were tested using the TaqPath™ COVID-19 triplex RT-qPCR kit (Thermo Fisher) according to the manufacturer's instructions. The SARS-CoV-2 genomic targets are located on the N, S, and Orf 1ab genes, with the MS2 bacteriophage serving as a control for extraction and reverse

transcription. The results were interpreted according to the recommendations of the TaqPath™ COVID-19 triplex CE-IVD kit. The presence of human DNA was validated by the detection of a signal for the ALB gene below 30 Ct. SARS-CoV-2 RT-qPCR (RT-qPCR) was carried out on foetal swabs (mouth, nasopharyngeal, mouth, stomach, bowel and anal), frozen placental samples (extraplacental membranes and basal plate), frozen foetal tissues (lung and the right kidney), formalin fixed and paraffin embedded (FFPE) and placental and foetal samples (thymus, lung, bronchial tree, stomach, spleen, adrenal gland, kidney, oesophagus, liver, heart, pancreas, and trachea) using an in-house real-time reverse transcription-PCR assay (47) to detect the emerging SARS-CoV-2 N501Y variants.

RT-dPCR

To improve the sensitivity of the detection of the SARS-CoV-2 genome, we used the IDNCOV-2d(s) kit (ID SOLUTIONS) on a Naica™ Crystal digital PCR system (Naica Geode and Naica Prism3; Stilla Technologies). Primers and double-labelled probes (hydrolysis probe) were designed in three specific regions of the SARS-CoV-2 viral RNA: N1 and N2 for the N gene and IP2 for the RdRP gene. Fluorescence signals were detected in the same FAM channel to increase the sensitivity and specificity of the test, and 3 droplets were theoretically emitted in the presence of one copy of the SARS-CoV-2 genome. A human gene measured in the HEX channel was used as an internal control to verify the presence of the sample. The reaction conditions were in accordance with the manufacturer's recommendations. According to the supplier, the limit of blank (LoB) values at 95% confidence of ARM-IDNCOV-2(s) and the limit of detection (LoD) are 2 and 6 droplets for N1+N2+IP2, respectively, and the same is true for endogenous.

Results

Placenta examination and results of SARS-CoV-2 testing

Macroscopic examination of the placenta revealed a diffusely distributed pattern of vertically oriented, firm trabeculae, lattice-like deposition of fibrin, with 6 cm subchorionic thrombosis and multiple intervillous thrombosis. During the microscopic examination, we observed prominent perivillous fibrin depositions with severe lymphohistiocytic intervillitis composed of CD4 lymphocytes, an increase in CD163- and CD68-positive macrophages and scarce MUM1-positive plasma cells. In addition, placental examination revealed trophoblastic necrosis with immunodetection of C4d and C5b-9 in the trophoblast layer. C4d and C5b-9 were negative on the control placenta (some of the decidual cells and a number of villi were positive amid perivillous fibrin deposition). Finally, brown staining of the trophoblast necrosis layer was performed using an antibody against the SARS-CoV-2 spike protein, and positive staining was observed on villous cytotrophoblast (VCT) syncytiotrophoblast (VST), in some fibroblastic-type and Hofbauer cells and on extravillous trophoblast cells (EVT) in the placental villi. We also noticed positivity for the SARS-CoV-2 envelope protein on some decidual capsular cells and granulocytes in the lumen of the umbilical vessels (*Figures 1 and 2*). Both RT-qPCR and RT-dPCR confirmed the abundance of SARS-CoV-2 in placental formalin-fixed and frozen specimens. The highest viral loads were detected in fixed formalin placental tissue (*Table 1*).

Foetal examination and results of SARS-CoV-2 testing

The foetus presented mild growth restriction, with biometrics close to 23 WG. The macroscopic examination of foetal organs revealed several petechial lesions on the liver surface, and some were found on the pleurae of the lower right and left lung lobes, along with the findings of mild cardiomegaly. The foetal brain was in an advanced state of lysis and was not removed. Microscopic

examination revealed adrenal, splenic and liver haemorrhages and the appearance of a “cardiac liver” with a subcapsular predominance (*Figures 3 and 4*). This resulted in significant sinusoidal dilatation with blood stasis and collapse of the hepatocyte trabeculae. The hepatocytes that were most affected in the subcapsular regions contained haemosiderin pigments. We also noted the presence of chronic hypoxic lesions with exaggerated haematopoiesis. There were also rare findings of emperipolesis in liver sinusoids without increased size or number of macrophages or clustering. No extrahepatic iron overload was observed on Perls Prussian blue stain. There were no inflammatory cells found in the foetal tissues. C5b-9 and C4d antibodies were negative on foetal samples that were labelled for those antibodies (liver and lung). Mouth, nasopharyngeal and stomach foetal swabs that were tested for SARS-CoV-2 were positive. SARS IHC on lung sections detected the SARS envelope protein within the desquamated cells in alveolar spaces, alveolar cells, fibroblasts and granulocytic cells, and the SARS envelope protein was also positive in stomach sections within the desquamated cells. The IHC for SARS-CoV-2 spike protein was positive on stomach samples within the cytoplasm of the stromal cells of the submucosae and the granulocytic cells. There was also positive staining of the SARS spike protein in macrophages of the liver and lymph node as well as in the cytoplasm of pericardium, endothelial and granulocytic cells in the heart samples (*Table 1*).

Both RT-qPCR and RT-dPCR confirmed the presence of SARS-CoV-2 in the foetal specimens (*Table 1*), including in lung tissue (FFPE and frozen), liver and spleen (FFPE), and trachea (frozen tissue), with almost equal viral loads. Only RT-PCR was able to highlight SARS-CoV-2 RNA in the thymus.

RT-qPCR of the placenta allowed us to exclude the original SARS-CoV-2 and 20I/501Y.V1. In-house-specific RT-qPCR allowed us to determine that the SARS-CoV-2 genotype was 20H/501Y. V2 (B1.351, Beta) variant (9).

Discussion

Here, we present a case of SARS-CoV-2 second trimester congenital infection with in utero foetal death (IUFD) secondary to extremely diffuse placental injuries characteristic of SARS-CoV-2 infection. There was a severely impaired maternal-foetal exchange, resulting in foetal hypoxia with heart failure and high levels of viral RNA in placental tissue. Our patient consulted one day before the IUD without indication for hospitalization. She presented a reduction in foetal movements and thrombocytopenia. The latter was associated with a 4.24-fold increased risk of inpatient mortality in a study from Wuhan (10).

Many authors have been interested in neonatal disease from mothers infected by SARS-CoV-2 (11–15). Vivanti and associates confirmed vertical transmission from mother to foetus and the possible consequences in the neonatal period (6).

Several authors (16–18) have described adverse outcomes in the mid- and late trimesters in pregnant women infected by SARS-CoV-2, but the biopsies of foetal tissues were all negative.

In this study, a congenital infection with an IUFD was diagnosed according to the proposed classification system of Prakesh S. Shah et al. (19). SARS-CoV-2 proteins and RNA have been detected in placental and some foetal samples using IHC, RT-qPCR and RT-dPCR assays (20–23). Indeed, we demonstrated the presence of SARS-CoV-2 viral RNA in pulmonary and liver foetal samples by the three previously described assays. Both RT-qPCR and RT-dPCR were positive in the spleen and trachea. IHC of the SARS-CoV-2 spike protein was positive in the stomach and heart samples, but we were unable to confirm the presence of viral RNA by the molecular assays used in these tissues.

SARS-CoV-2 uses the SARS-CoV receptor angiotensin-converting enzyme 2 (ACE2) for entry and the serine protease TMPRSS2 for S protein priming. The expression of virus receptors in foetal target organs (main tissues: foetal heart, lung, liver) is one of the determining factors for foetal

vulnerability to SARS-CoV-2 (24-28). In our case, there was no immunodetection of viral RNA on cardiomyocytes, which are the major functional cells of the heart, and no segmental or histological anomalies were noted on the heart sections. We noted several liver lesions and the presence of SARS-CoV-2 through IHC and molecular assays. The appearance of a “congested liver secondary to congestive heart failure” in addition to cardiomegaly were arguments for the presence of heart failure. Such injuries were more likely due to foetal hypoxia secondary to severely impaired maternal-foetal exchange than a direct effect of the virus itself. However, the virus might have contributed to cardiac failure, as it was detected in situ (granulocytes and endothelial and pericardium cells) (28). An additional argument to support our theory is that both SARS-CoV-2 RT-qPCR and RT-dPCR assays were negative on FFPE kidney samples. In fact, unlike adult human kidney tissue, in which ACE2 is highly expressed, ACE2 is not expressed in the foetal kidney, whereas TMPRSS2 is moderately expressed (28).

We did not find any diffuse alveolar damage (DAD) in lung specimens, unlike what has been widely described in COVID-19 adults (29). In some studies, SARS-CoV-2 virions were detected within both type 1 and type 2 pneumocytes in human adult pulmonary samples (30). In our case study, we observed viral RNA in alveolar-type cells with the anti-SARS envelope antibody, but the anti-SARS-CoV-2 spike protein antibody was not detected in type 1 or type 2 pneumocytes. To the best of our knowledge, there is no available atlas of human foetal lungs (28). However, in the murine lung cell atlas, both ACE2 and TMPRSS2 are highly expressed in airway epithelial cells and endothelial cells, more highly than in alveolar cell types, from the late pregnancy stage to the earliest postnatal days and decrease thereafter (31). The detection of SARS-CoV-2 viral envelope protein on alveolar cells of the foetal lung tissue with absence of expression on respiratory cells in this second trimester IUD case study could suggest variability of ACE2 and TMPRSS2 expression on different lineage lung cells

between the second and last trimester of pregnancy, since the gestational age in our case was 24⁺² WG.

Regarding placental lesions, our findings are similar to those reported in the literature (32–35), with massive perivillous fibrin depositions with chronic lymphohistiocytic intervillitis and trophoblastic cell necrosis. The combination of the latter two lesions was strongly suggestive of SARS-CoV-2 vertical transmission (36,37). IHC revealed that the inflammatory infiltrate was composed mostly of CD163- and CD68-positive macrophages, as previously reported in the literature (37,38), with numerous CD4-positive T cells. Moreover, in this case study, we detected the presence of complement (C) deposition, C5b-9 and C4d, on necrotic and virus-infected trophoblastic cells, unlike on foetal liver and lung samples and controls. Some authors found that lung deposits of C with IgG displayed a similar even distribution. In the present case, IUD occurred seven days after the onset of symptoms. Given that SARS-CoV-2 IgG antibodies were detected on days 0–7 and increased on days 8–14 (39), it is possible that the production of maternal SARS-CoV-2 IgG in the case of placental passage of IgG could occur in cases of transplacental transmission of SARS-CoV-2 to activate C pathway formation of the membrane attack complex on trophoblastic cells and induce injury and necrosis. Vascular C deposition could be used as a marker to monitor the progression of disease (40).

We identified the presence of SARS-CoV-2 viral proteins within the villous, VCT, VST, stromal and EVT cells, which express the ACE2 gene based on SARS-CoV-2 RNA-sequencing data from an early human placenta (first trimester) (28). The ACEm RNA levels were highest in term placentae, with an increasing expression of ACE2 in EVT at 24 weeks (28,41), corresponding to the term IUFD case that we report here. Knowing that placental function is mainly regulated by villous and EVT cells, we

suppose that the latter could play a major role in the pathogenesis of SARS-CoV-2 infection in placental tissue in the second trimester.

The occurrence of this condition leads to more questions than answers: should we modify the monitoring of patients infected with SARS-CoV-2, and should we consult the emergency room for obstetrical symptomatology as described in our situation? Compared with other well-known congenital infections, could the severity of the antenatal clinical manifestations of SARS-CoV-2-related disease be correlated with the gestational age of onset of the congenital infection? Finally, we should incriminate this adverse outcome at 20H/501Y. The V2 (B1.351, Beta, South African) variant was identified in our case, but does it concern all of the known variants? More studies and more hindsight are needed to answer all of these questions.

In conclusion, we present a case of SARS-CoV-2 second trimester congenital infection with IUD secondary to extremely diffuse placental injuries. The involvement of certain variants in the poor prognosis of pregnancy outcomes remains undetermined. Emergency obstetrical management of pregnant women in cases of suspected vertical transmission of SARS-CoV-2 should be considered, especially in the presence of reduced foetal movement with thrombocytopenia.

NOTES

Authors' contributions

E. L, R. F and J. T performed the macroscopic and microscopic examinations and wrote the majority of the study.

F. F participated in the development of the RT-dPCR kit, performed the assays and wrote the corresponding parts.

C. Z and C. G performed the RT-qPCR and extraction of the viral RNA.

S. C. performed additional immunochemistry experiments and brought pathological expertise for the interpretation of the results obtained. They reviewed and corrected the manuscript.

D.F. B and J. B reviewed and corrected the manuscript

H. L, L. participated by offering their anatomopathological expertise to the whole study.

F. B brought their obstetrical expertise to the whole study.

D. S is the obstetrician who ensured the medical follow-up of the patient.

S. M, M.O. I and J.L. M participated in the immunological and virological explorations.

Acknowledgements

We would like to thank the technicians of the pathology laboratory of the Timone Hospital who allowed the realization of the usual techniques and immunohistochemistry, Dr. C. DETEIL for having contributed to the development of the anti SARS-CoV antibodies in the laboratory, and Professor D. FIGARELLA-BRANGER for reviewing the manuscript.

Ethics declaration

Written informed consent was obtained from the woman for the publication of this report. According to French regulations, institutional review board (IRB) approval is not required for case reports, provided that the patient's written consent is obtained. The French Ethical Committee for Research in Obstetrics and Gynaecology reviewed the work and confirmed that IRB approval was unnecessary. The case study was performed in agreement with the principles of the Declaration of Helsinki and CARE guidelines.

Funding source

This study did not receive any specific financial support.

Conflict of interest

F. F is the scientific director and founding partner of ID SOLUTIONS and reports ID SOLUTIONS, DM-DIV manufacturing company (Grabels, 34790 FRANCE) has developed, produced and provides free of charge the dPCR kits.

References

1. Di Mascio D, Buca D, Berghella V, Khalil A, Rizzo G, Odibo A, et al. Counseling in maternal-fetal medicine: SARS-CoV-2 infection in pregnancy. *Ultrasound Obstet Gynecol.* 2021 May;57(5):687-697
2. Mullins E, Hudak MI, Banerjee J, Getzlaff T, Townson J, Barnette K, et al. Pregnancy and neonatal outcomes of COVID-19: coreporting of common outcomes from PAN-COVID and AAP-SONPM registries. *Ultrasound Obstet Gynecol Off J Int Soc Ultrasound Obstet Gynecol.* 2021 Apr;57(4):573-581
3. Chen H, Guo J, Wang C, Luo F, Yu X, Zhang W, et al. Clinical characteristics and intrauterine vertical transmission potential of COVID-19 infection in nine pregnant women: a retrospective review of medical records. *Lancet Lond Engl.* 2020 Mar 7;395(10226):809-815
4. Kotlyar Am, Grechukhina O, Chen A, Popkhadze S, Grimshaw A, Tal O, et al. Vertical transmission of coronavirus disease 2019: a systematic review and meta-analysis. *Am J Obstet Gynecol.* 2021 Jan;224(1):35-53.e3
5. Schwartz Da, Morotti D, Beigi B, Moshfegh F, Zafaranloo N, Patanè L. Confirming Vertical Fetal Infection With Coronavirus Disease 2019: Neonatal and Pathology Criteria for Early Onset and Transplacental Transmission of Severe Acute Respiratory Syndrome Coronavirus 2 From Infected Pregnant Mothers. *Arch Pathol Lab Med.* 2020 Dec 1;144(12):1451-1456
6. Vivanti AJ, Vauloup-Fellous C, Prevot S, Zupan V, Suffee C, Do Cao J, et al. Transplacental transmission of SARS-CoV-2 infection. *Nat Commun.* 2020 Jul 14;11(1):3572
7. Protocole_examen_autopsique_foetal_neonatal_cd_20140528_vd.pdf

8. Maroun LI, Graem N. Autopsy standards of body parameters and fresh organ weights in nonmacerated and macerated human fetuses. *Pediatr Dev Pathol Off J Soc Pediatr Pathol Paediatr Pathol Soc.* Mar-Apr 2005;8(2):204-17
9. Bedotto M, Fournier Pe, Houhamdi L, Colson P, Raoult D. Implementation of an in-house real-time reverse transcription-PCR assay to detect the emerging SARS-CoV-2 N501Y variants. *J Clin Virol Off Publ Pan Am Soc Clin Virol.* 2021 Jul;140:104868
10. Liu Y, Sun W, Guo Y, Chen L, Zhang L, Zhao S, et al. Association between platelet parameters and mortality in coronavirus disease 2019: retrospective cohort study. *Platelets.* 2020 May;31(4):490–6.
11. Juan J, Gil Mm, Rong Z, Zhang Y, Yang H, Poon Lc. Effect of coronavirus disease 2019 (COVID-19) on maternal, perinatal and neonatal outcome: systematic review. *Ultrasound Obstet Gynecol Off J Int Soc Ultrasound Obstet Gynecol.* 2020 Jul;56(1):15-27
12. Schwartz Da. An Analysis of 38 Pregnant Women With COVID-19, Their Newborn Infants, and Maternal-Fetal Transmission of SARS-CoV-2: Maternal Coronavirus Infections and Pregnancy Outcomes. *Arch Pathol Lab Med.* 2020 Jul 1;144(7):799-805
13. Schwartz Da. The Effects of Pregnancy on Women With COVID-19: Maternal and Infant Outcomes. *Clin Infect Dis Off Publ Infect Dis Soc Am.* 2020 Nov 19;71(16):2042-2044
14. Yu N, Li W, Kang Q, Xiong Z, Wang S, Lin X, et al. Clinical features and obstetric and neonatal outcomes of pregnant patients with COVID-19 in Wuhan, China: a retrospective, single-centre, descriptive study. *Lancet Infect Dis.* 2020 May;20(5):559-564
15. Kimberlin Dw, Stagno S. Can SARS-CoV-2 Infection Be Acquired In Utero?: More Definitive Evidence Is Needed. *JAMA.* 2020 May 12;323(18):1788-1789

16. Zhang Y, Zheng L, Liu L, Zhao M, Xiao J, Zhao Q. Liver impairment in COVID-19 patients: A retrospective analysis of 115 cases from a single centre in Wuhan city, China. *Liver Int Off J Int Assoc Study Liver*. 2020 Sep;40(9):2095-2103
17. Baud D, Greub G, Favre G, Gengler C, Jaton K, Dubruc E, et al. Second-Trimester Miscarriage in a Pregnant Woman With SARS-CoV-2 Infection. *JAMA*. 2020 Jun 2;323(21):2198-2200
18. Richtmann R, Torloni Mr, Oyamada Otani Ar, Levi Je, Crema Tobará M, de Almeida Silva C, et al. Fetal deaths in pregnancies with SARS-CoV-2 infection in Brazil: A case series. *Case Rep Womens Health*. 2020 Jul 12;27:e00243
19. Shah Ps, Diambomba Y, Acharya G, Morris Sk, Bitnun A. Classification system and case definition for SARS-CoV-2 infection in pregnant women, fetuses, and neonates. *Acta Obstet Gynecol Scand*. 2020 May;99(5):565-568
20. Wang W, Xu Y, Gao R, Lu R, Han K, Wu G, et al. Detection of SARS-CoV-2 in Different Types of Clinical Specimens. *JAMA*; 2020 May 12;323(18):1843-1844
21. Suo T, Liu X, Feng J, Guo M, Hu W, Guo D, et al. ddPCR: a more accurate tool for SARS-CoV-2 detection in low viral load specimens. *Emerg Microbes Infect*. 2020 Dec;9(1):1259-1268
22. Dong L, Zhou J, Niu C, Wang Q, Pan Y, Sheng S, et al. Highly accurate and sensitive diagnostic detection of SARS-CoV-2 by digital PCR. *Talanta*. 2021 Mar 1;224:121726
23. Baretts D, Appay R, Heinisch M, Battistella M, Bouvier C, Chotard G, et al. Specific and Sensitive Diagnosis of BCOR-ITD in Various Cancers by Digital PCR. *Front Oncol*. 2021 Feb 25;11:645512
24. Zhou P, Yang Xi, Wang Xg, Hu B, Zhang L, Zhang W, et al. A pneumonia outbreak associated with a new coronavirus of probable bat origin. *Nature*. 2020 Mar;579(7798):270-273
25. Komine-Aizawa S, Takada K, Hayakawa S. Placental barrier against COVID-19. *Placenta*. 2020

Sep;99:45–9.

26. Hoffmann M, Kleine-Weber H, Schroeder S, Krüger N, Herrler T, Erichsen S, et al. SARS-CoV-2 Cell Entry Depends on ACE2 and TMPRSS2 and Is Blocked by a Clinically Proven Protease Inhibitor. *Cell*. 2020 Apr 16;181(2):271-280.e8
27. Shang J, Ye G, Shi K, Wan Y, Luo C, Aihara H, et al. Structural basis of receptor recognition by SARS-CoV-2. *Nature*. 2020 May;581(7807):221-224
28. Li M, Chen L, Zhang J, Xiong C, Li X. The SARS-CoV-2 receptor ACE2 expression of maternal-fetal interface and fetal organs by single-cell transcriptome study. *PloS One*. 2020 Apr 16;15(4):e0230295
29. Rimmelink M, De Mendonça R, D’Haene N, De Clercq S, Verocq C, Lebrun L, et al. Unspecific post-mortem findings despite multiorgan viral spread in COVID-19 patients. *Crit Care Lond Engl*. 2020 Aug 12;24(1):495
30. Carsana L, Sonzogni A, Nasr A, Rossi Rs, Pellegrinelli A, Zerbi P, et al. Pulmonary post-mortem findings in a series of COVID-19 cases from northern Italy: a two-centre descriptive study. *Lancet Infect Dis*. 2020 Oct;20(10):1135-1140
31. Khoury Ee, Knaney Y, Fokra A, Kinaneh S, Azzam Z, Heyman Sn, et al. Pulmonary, cardiac and renal distribution of ACE2, furin, TMPRSS2 and ADAM17 in rats with heart failure: Potential implication for COVID-19 disease. *J Cell Mol Med*. 2021 Apr;25(8):3840-3855
32. Gulersen M, Prasannan L, Tam Tam H, Metz Cn, Rochelson B, Meirowitz N, et al. Histopathologic evaluation of placentas after diagnosis of maternal severe acute respiratory syndrome coronavirus 2 infection. *Am J Obstet Gynecol*. 2020 Nov;2(4):100211
33. Komine-Aizawa S, Takada K, Hayakawa S. Placental barrier against COVID-19. *Placenta*. 2020 Sep 15;99:45-49

34. Schwartz DA, Morotti D. Placental Pathology of COVID-19 with and without Fetal and Neonatal Infection: Trophoblast Necrosis and Chronic Histiocytic Intervillositis as Risk Factors for Transplacental Transmission of SARS-CoV-2. *Viruses*. 2020 Nov 15;12(11):1308.
35. Shanes ED, Mithal LB, Otero S, Azad HA, Miller ES, Goldstein JA. Placental Pathology in COVID-19. *Am J Clin Pathol*. 2020 Jun 8;154(1):23–32.
36. Taglauer E, Benarroch Y, Rop K, Barnett E, Sabharwal V, Yarrington C, et al. Consistent localization of SARS-CoV-2 spike glycoprotein and ACE2 over TMPRSS2 predominance in placental villi of 15 COVID-19 positive maternal-fetal dyads. *Placenta*. 2020 Oct;100:69–74.
37. Hosier H, Farhadian Sf, Morotti Ra, Deshmukh U, Lu-Culligan A, Campbell Kh, et al. SARS-CoV-2 infection of the placenta. *J Clin Invest*. 2020 Sep 1;130(9):4947-4953
38. Pulinx B, Kieffer D, Michiels I, Petermans S, Strybol D, Delvaux S, et al. Vertical transmission of SARS-CoV-2 infection and preterm birth. *Eur J Clin Microbiol Infect Dis Off Publ Eur Soc Clin Microbiol*. 2020 Dec;39(12):2441-2445
39. Chouaki Benmansour N, Carvelli J, Vivier É. Implication de la cascade du complément dans les formes sévères de COVID-19. *médecine/sciences*. 2021 Apr;37(4):333–41.
40. Macor P, Durigutto P, Mangogna A, Bussani R, D'Errico S, Zanon M, et al. Multi-organ complement deposition in COVID-19 patients. 2021 Jan;2021.01.07.21249116
41. Risitano Am, Mastellos Dc, Huber-Lang M, Yancopoulou D, Garlanda C, Ciceri F, et al. Complement as a target in COVID-19? *Nat Rev Immunol* 2020 Jun;20(6):343-344

Sample		SARS-CoV-2 immunochemistry <i>(SARS-CoV-2 spike protein and/or SARS-CoV-2 envelope protein)</i>	SARS-CoV-2 genome detection	
			RT-qPCR <i>(ct)</i>	RT-dPCR <i>(status/positive droplet>4)</i>
Swabs				
Mother	Nasopharyngeal	NA	+	NA
Foetal	Nasopharyngeal		+/33	
	Mouth		+/32,0	
	Stomach		+	
	Bowel		-	
	Anal		-	
Placenta				
Formalin fixed	Extra placental membranes	+ <i>(decidua capsularis, granulocytic cells: umbilical vessels)</i>	+/33,8	NA
	Placental tissue	+ <i>(VCT necrotic cells and VST, basement membrane, fibroblastic stromal cells of villi, Hofbauer cells and EVT)</i>	+/18,8 variant RT- PCR	+/>20.000
Frozen tissue	Extra placental membranes	NA	+/33,8	+/596
	Placental tissue		+/25,9	+/>20.000
Foetal Tissues				
Formalin	Lung	+ <i>(desquamated cells, alveolar type,</i>	+/34,6	+/8

fixed		<i>fibroblastic and granulocytic, cells)</i>		
	Liver	+ <i>(macrophages)</i>	+/33	+/6
	Stomach	+ <i>(desquamated cells, stromal cells of sub mucosae and granulocytic cells)</i>	-	-
	Lymphatic node (perigastric)	+ <i>(lymphocytes)</i>	NA	NA
	Heart	+ <i>(endothelial cells, granulocytes and the pericardial surface)</i>	-	-
	Spleen	NA	+/34,7	+/8
	Thymus		+/32,8	-
	Adrenal gland		-	-
	Kidney		-	-
Frozen tissue	Lung	NA	+/35	+/21
	Stomach		-	NT
	Trachea		+/34,5	+/5
	Kidney		-	borderline/4

Table 1: Summary of the results of SARS-CoV-2 testing with various detection techniques (“+” positive result; “-” negative result; “NA” tissue not available; RT-QPCR: real-time polymerase chain reaction; RT-dPCR: digital polymerase chain reaction). Villous cytotrophoblast cells (VCT), villous syncytiotrophoblast cells (VST), extravillous trophoblast cells (EVT).

Figure Legends

Figure 1: Microscopic examination of the placenta: **(a)** Lymphohistiocytic inter villitis with trophoblast cell necrosis (x20); **(b)** Immunodetection of C4d and **(c)** C5b9 in the trophoblast layer (x20); **(d)** Brown staining of the trophoblast layer using an antibody to SARS-CoV-2 spike protein (x20); **(e)** Positive staining in syncytiotrophoblast as well as fibroblastic-type cells in the placental villi **(f)** using an antibody to SARS-CoV-2 envelope protein (x40);

Figure 2 : Microscopic examination of the placenta : **(a)** Positive staining in Hofbauer cells with SARS-CoV-2 envelope protein (x20); **(b)** Extravillous trophoblastic cell labelling with spike protein antibody, **(c)** placental control: negativity with SARS-CoV-2 spike protein in 22 GW. **(d)** Immunohistochemistry revealed that the inflammatory infiltrate was composed mostly of CD4-positive T-cells together with an increase in CD163-positive macrophages **(e); (f)** Scarce MUM1-positive plasma cells (x20) **(l)**.

Figure 3: Microscopic examination of fetal specimens: **(a)** Liver hemorrhage with appearance of “cardiac liver” of a sub capsular predominance on Trichrome stain; **(b)** exaggerated hematopoiesis; **(c)** Histiocyte showing emperipolesis (arrow) in the liver tissue (x40) with CD 163 antibodies; **(d)** Perls Prussian blue stained section of liver fetal tissue showing hemosiderosis (x20) ; **(e)** Negative fetal liver control SARS-CoV2 spike protein (x20); **(f)** Brown staining of the infected liver macrophages using an antibody to SARS-CoV-2 spike protein (x20)

Figure 4 : Microscopic examination of fetal specimens : **(a)** Intense brown cytoplasmic positivity of alveolar (arrow) cells on the fetal lung (x40); **(b)** desquamated cells using an antibody to SARS-CoV-2 spike protein in an alveolar lumina (x40); **(c)** Heart specimen: staining of the SARS Cov-2 antibody-spike protein on granulocytes (arrow) **(d)** Staining of the SARS-CoV-2 spike protein on the pericardial surface (x40); **(e)** Brown staining of fibroblastic (red arrow) and granulocytic cells (black arrow) of stomach mucosae using an antibody to SARS-CoV-2 spike protein (x4); **(f)** Positivity of SARS-CoV-2 spike protein expression on a perigastric lymph nodes.

Figure 1

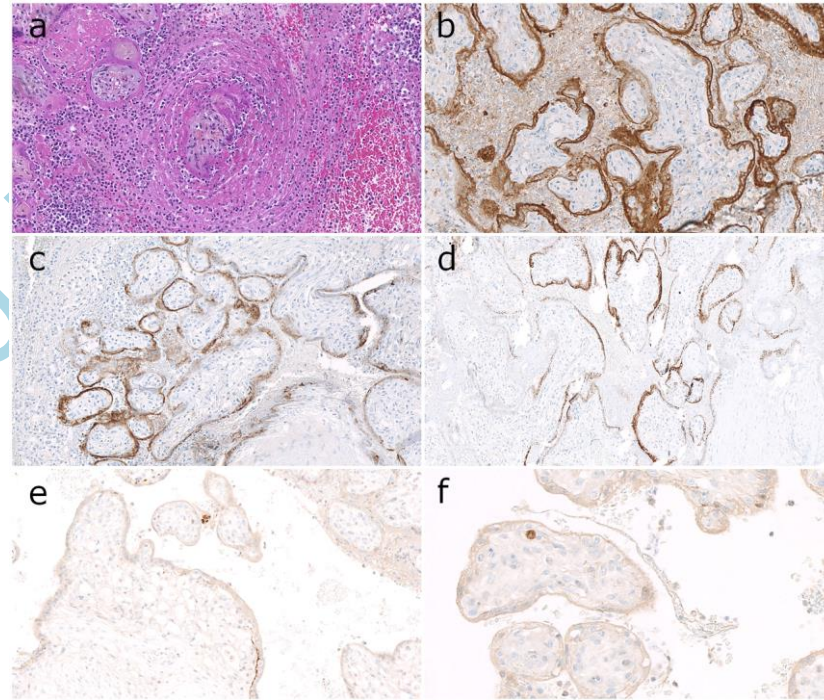


Figure 2

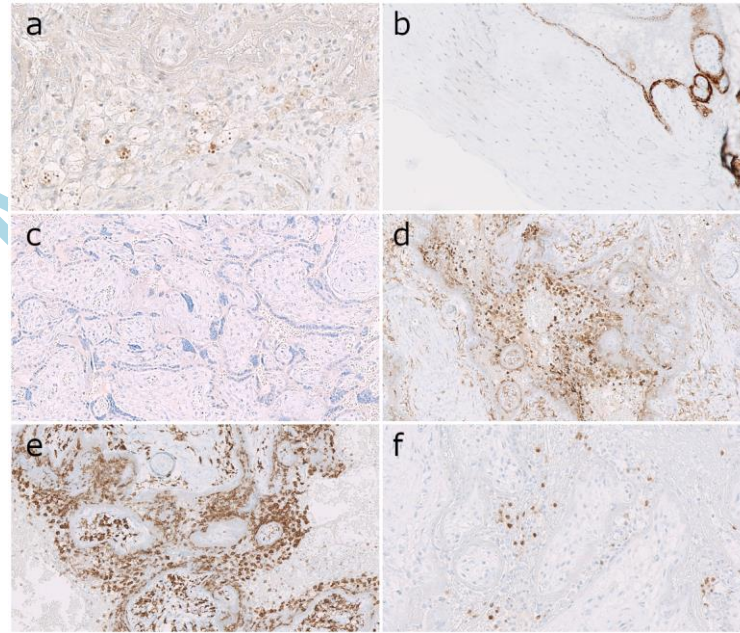


Figure 3

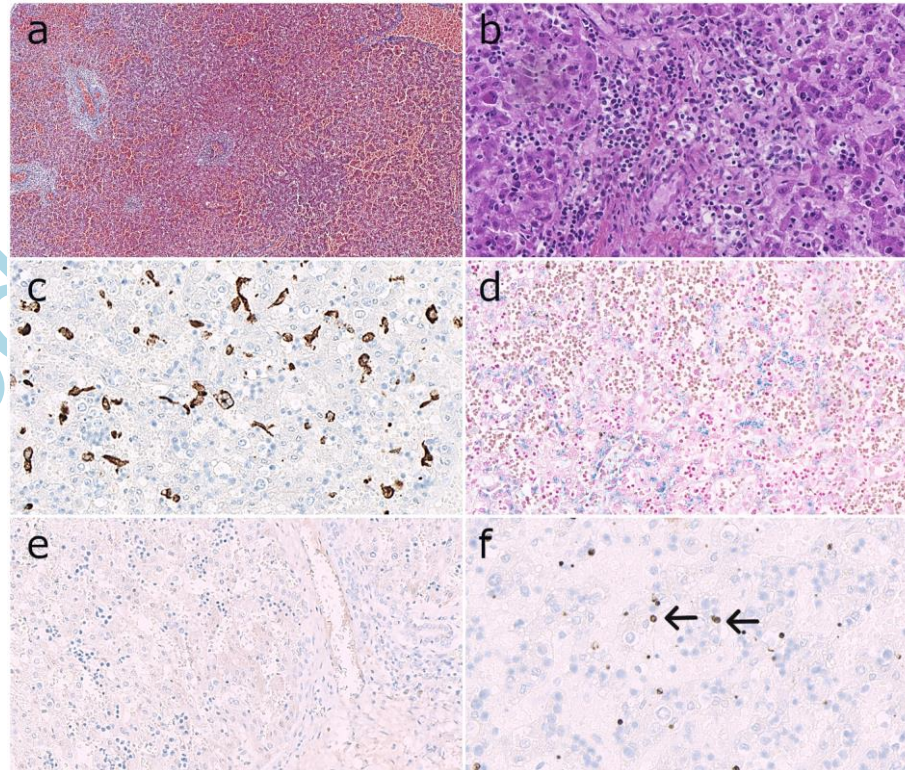


Figure 4

